# Examination of the Performance Characteristics of Velostat as an In-Socket Pressure Sensor

Matthew Hopkins, Ravi Vaidyanathan, Member, IEEE and Alison H. McGregor

***Abstract*—Velostat is a low-cost, low-profile electrical bagging material with piezoresistive properties, making it an attractive option for in-socket pressure sensing. The focus of this research was to explore the suitability of a Velostat-based system for providing real-time socket pressure profiles. The prototype system performance was explored through a series of bench tests to determine properties including accuracy, repeatability and hysteresis responses, and through participant testing with a single subject. The fabricated sensors demonstrated mean accuracy errors of 110 kPa and significant cyclical and thermal drift effects of up to 0.00715 V/cycle and leading to up to a 67% difference in voltage range respectively. Despite these errors the system was able to capture data within a prosthetic socket, aligning to expected contact and loading patterns for the socket and amputation type. Distinct pressure maps were obtained for standing and walking tasks displaying loading patterns indicative of posture and gait phase. The system demonstrated utility for assessing contact and movement patterns within a prosthetic socket, potentially useful for improvement of socket fit, in a low cost, low profile and adaptable format. However, Velostat requires significant improvement in its electrical properties before proving suitable for accurate pressure measurement tools in lower limb prosthetics.**

***Index Terms*— Piezoresistive measurement, pressure sensing, prosthetics, prosthetic fitting, Velostat, wearable sensors.**

## I. Introduction

UP to 185,000 people experience major limb amputation annually within the USA; a figure predicted to rise due to increased prevalence of diseases such as diabetes [1–4]. Recent conflicts in Afghanistan and Iraq have contributed further individuals, often with numerous injuries and multiple amputations to the affected population [5, 6]. Whilst significant technological advancement has been achieved with regards to prostheses through the introduction of sophisticated microprocessor-controlled joints [7, 8], relatively little improvement has been made to the prosthetic socket [9].

In a study by Nielson, 52% of the lower limb amputees surveyed stated that comfort was their most important concern, this was above other factors including functionality of the prosthesis [10]. Not surprisingly, the socket is frequently cited as the most important factor for user comfort and acceptance of the prosthetic limb [11, 12].

The socket is a hostile environment in which the skin of the residual limb is exposed to normal and shear stresses, elevated temperature, trapped moisture and sustained exposure to the chemical compounds of the prosthesis [13, 14]. Consequently, amputees may experience discomfort, tissue breakdown and development of numerous conditions such as blisters, stump oedema and skin carcinoma [4, 11, 13–18]. In the worst case, chronic ulceration and associated infection can lead to re-amputation of the limb, further restricting functionality [19].

Socket interface pressure is influenced by a number of factors including shape, alignment, liner material, the suspension system used, componentry and the nature of the ambulation task [4, 17]. Prosthetists aim to control loading through alteration of the shape and form of the socket; however, they must rely on experience [9, 11], intuition [20] and the amputee's reports of comfort which may be compromised due to the medical causes underpinning the amputation.

There is a strong demand for a greater biomechanical understanding of the internal environment of the prosthetic socket, particularly with regards to the interfacial stress profile between the residual limb and the socket, to reduce occurrence of injury and improve acceptance rates of the prosthetic limb [13]. Crucial to this understanding are factors such as distribution, magnitude and direction of load in accordance with the soft tissue responses [13].

Attempts to produce sensors capable of measuring the pressure within prosthetic sockets have tended to involve piezoresistive [21–23], piezoelectric [24–26], capacitive [27–30], optical sensors [31–37] and microelectromechanical (MEMs) sensors [38–41].

Piezoresistive sensors have been made commercially available through manufacturers such as Tekscan and Rincoe in the form of force sensitive resistors (FSRs) [21–23]. These sensors are low profile, making them ideal for insertion in the socket, however, cost may be a barrier to application [22].

Piezoelectric sensors demonstrate high sensitivity, a good high-frequency response and do not require a power source, however, their large internal resistance compromises their

Manuscript received August 05, 2019. This work was supported by the Royal British Legion Centre for Blast Injury Studies.

M. Hopkins is with the Sackler MSk Laboratory, Department of Surgery and Cancer, Imperial College London, London, W12 0BZ, United Kingdom (e-mail: matthew.hopkins@imperial.ac.uk).

R. Vaidyanathan is with the Biomechatronics laboratory, Department of Mechanical Engineering, Imperial College London, SW7 2AZ, United Kingdom (e-mail: r.vaidyanathan@imperial.ac.uk).

A. H. McGregor is with the Sackler MSk Laboratory, Department of Surgery and Cancer, Imperial College London, London, W12 0BZ, United Kingdom (e-mail: a.mcgregor@imperial.ac.uk)..

ability to detect static forces [42, 43].

Capacitive sensors offer high dynamic range, good linearity, good hysteresis and drift characteristics, and are able to measure normal and shear stress [11, 30, 44]. Drawbacks include non-negligible crosstalk limiting their arrangement in arrays, the requirement for complex circuitry and manufacturing costs [11, 45].

Optical sensors have been produced by several groups in the form of optical Fibre-Bragg Gratings (FBGs) or optoelectronic sensors. FBGs have distinct advantages including biocompatibility, immunity to electromagnetic interference (EMI), self-referencing enabled through wavelength encoding and linear dependence on temperature and shear [46, 47]. Despite these factors, they require extensive multidisciplinary expertise to operate and require large and bulky detectors [47]. Optoelectronic sensors are capable of measuring both normal and shear stresses and being produced using surface mount components allows them to be easily integrated with printed circuit boards [11, 36, 37, 45]. Unlike FBG sensors, optoelectronic devices are susceptible to EMI and may sustain damage to the electronic components [11, 45].

MEMs sensors have been applied to lower limb prosthetics by a handful of researchers either as bespoke units [38, 40] or through use of commercially available designs [39]. MEMs devices offer compact [38], low-cost [41] solutions to stress measurement. Typically, these sensors exhibit high linearity [38], good drift characteristics [39] and are largely unaffected by noise [41]. Sensors may be arranged to measure both normal and shear forces [38, 40, 41]. However, issues with hysteresis have been noted [38, 39] and limited application has been presented to clinical scenarios [40].

The objective of this research was to produce a low-cost, low-profile sensing device for use within lower limb prosthetic limbs to quantify pressure distribution in real time. The material used for this device was Velostat, a thin film material comprised of carbon-impregnated polyolefin [48–51]. Due to its low-cost and piezoresistive properties it offers an attractive sensing solution. The use of Velostat has been explored in the literature with regards to applications such as human movement monitoring [48, 52], control of pressure redistributing insoles [49], sitting posture monitoring [53, 54], quantification of hand forces [55], assessment of psychomotor development in children [56], finger gesture recognition [51] and neonatal monitoring [57]. The performance of the material with regards to properties such as linearity, hysteresis and repeatability appears to vary based on application and the loading environment, suggesting review is necessary per application [52, 55, 58, 59]. To our knowledge, application of this material has not been explored with regards to lower-limb prosthetics with the exception of a US patent filed regarding a sensor filled strut-socket design [50].This paper describes a method for manufacture of these devices and their performance as observed under mechanical bench tests.

## II. Sensor Design

A thin, flexible and customisable piezo-resistive sensor was developed based on Velostat in order to transduce surface contact pressure. The sensor structure employs two circuitry layers sandwiching a pressure sensitive Velostat element [see Fig. 1]. The sensor design was centred around minimising size and cost, and providing a discrete and portable sensing solution. As such, the construction utilizes readily available materials.

The core of the sensor is piezo-resistive, 0.06 mm thick Velostat with a diameter of 5 mm. Fig. 2 shows a scanning electron microscope (SEM) image of a sample of the Velostat material used in sensor construction. As force is applied to the material its resistance falls due to micro-Brownian motion of the carbon filler particles in the polymer matrix [49, 58–60]. The sensors form part of a voltage divider circuit, used to minimise the required circuitry components required on the accompanying printed circuit board (PCB). The output voltage of the circuit is given by (1), where $V_{out}$ is the output voltage, $V_{in}$ is the input voltage and $R_1$ and $R_2$ are resistance values of the sensor and pull-down resistor respectively.

$$V_{out} = V_{in}\left(\frac{R_2}{R_1 + R_2}\right) \quad (1)$$

Piezoresistive elements were arranged in a matrix and multiplexing was utilised to reduce wiring requirements. The form of the matrix was strips of twelve sensitive elements arranged sequentially along the longitudinal direction of the strip [see Fig. 3]. Six voltage input lines were arranged on the upper circuitry layer, supplying adjacent pairs of sensors. The lower circuitry layer consisted of two output lines alternating between sensitive elements from the distal-most end to the proximal-most end. Electrode plates 2 mm in diameter were positioned 20 mm apart from one another along the strip and used as the contact point for each sensitive element. Velostat was sandwiched between the twelve pairs of electrodes on the upper and lower circuitry layers. The remaining areas of the circuitry were insulated from one another with an adhesive layer to prevent short circuits. A pull-down resistor of 1 kΩ was used to complete the instrumentation circuit. Diodes were added to the current supply lines to avoid crosstalk between sensors. The sensors attached to a bespoke printed circuit board with a microcontroller unit, inertial measurement unit (IMU) and Bluetooth module for data acquisition and transfer.

## III. Sensor Fabrication

Sensor manufacture was achieved using printed circuit board development techniques, which follow a process of circuitry design, circuitry production and sensor lay-up. Circuitry designs were printed directly onto sheets of copper using a Xerox ColorQube solid ink printer. The wax-based ink provides clean and consistent coverage of the tracks leaving the surrounding excess copper exposed. The copper was then backed with a sheet of acetate using double-sided adhesive. Exposed copper was removed using a heated bubble-etch tank filled with sodium persulfate solution. After 30 minutes of exposure, the sheet was removed and cleaned with acetone. Both sides of the circuitry were then used to sandwich Velostat elements using a central adhesive layer.

## IV. Experimental Evaluation

### A. Bench Tests

Sensor performance characteristics were determined using the compressive loading of a mechanical test system (MecMesin, 10kN load cell) with a customised load application adapter. The adapter is comprised a 3D printed column fitted with a syringe, attached to a barometric pressure sensor [see Fig. 4]. The sensor allowed chamber pressure to be recorded in real time, coinciding with the loading of the flexible sensors. The plunger of the syringe was modified with a 3D printed attachment equal in diameter to the syringe chamber. Use of the adapter was made necessary due to the poor load control offered by the system at low Newton values. The experiments focused on sensor response characteristics for distinct load levels, continuous cyclical loads, drift characteristics and variation due to loading rate changes. Sensors were loaded between the thresholds of 0 and 400 kPa, determined through the literature as the expected range in which pressures may manifest within lower limb prosthetic sockets [4, 16, 61].

An initial measure of sensor resistance characteristics was performed by loading three sensors with discrete loads between 0 and 400 kPa at intervals of 40 kPa. Sensor accuracy was observed through application of 20 cyclical loads between 0 and 400 kPa from which a calibration relationship was fitted, followed by discrete loading thresholds between 0 and 400 kPa at intervals of 40 kPa. Linearity was examined through inspection of the loading response for ten sensors subject to cyclical loading between 0 and 400 kPa. A total of 20 cycles were performed at a loading rate of 1000 mm/min. Additional tests were performed at 500 mm/min to determine the effect of loading rate.

Repeatability was defined as the difference in output produced when each sensor was loaded to the same pressure. Three sensors were loaded between 0 and 400 kPa for 200 cycles each. Sensors were tested on both a solid and compliant surface.

Hysteresis was defined as the maximum difference in output for a single load when loading and unloading. The error was calculated as a percentage of the full-scale output (FSO) [see (2)].

$$Hysteresis(\%) = \left|\frac{V_{load} - V_{unload}}{V_{max} - V_{min}}\right| \cdot 100\% \quad (2)$$

Where $V_{load}$ and $V_{unload}$ are the sensor voltages corresponding to the greatest difference between the loading and unloading responses, and where $V_{max}$ and $V_{min}$ are the sensor voltages at maximum and minimum load respectively. Hysteresis was determined under cyclical loading of the sensors. Six sensors were subjected to 20 cycles at a loading rate of 1000 mm/min between 0 and 400 kPa.

Drift was defined as a change in sensor output, generally an increase in value, over time for a given load. Four sensors were loaded to values of approximately 25 kPa, 100 kPa, 200 kPa and 300 kPa, with loads held for five minutes.

The effect of elevated temperature on the response of the sensors was explored by heating the sensors with a hot-plate [see Fig. 4] to temperatures of 20°C, 30°C and 40°C. These thresholds were chosen based on body temperature values found in the literature [62–65]. At these temperatures, sensor response was observed for approximately 30 minutes at zero-load and subsequently, over 20 cycles at a loading rate of 1000 mm/min between 0 and 400 kPa.

### B. Participant Evaluation

The performance of the sensors was explored via application of a total of 12 sensor strips, each containing 12 individual sensing elements spaced 2cm apart, to the interior of a participant's above-knee socket (ethical approval received from NRES Committee London-Riverside, REC reference: 15/LO/1633, IRAS project ID: 177122). The participant was a bilateral amputee with the instrumented socket on their right residual limb [see Table 1 for full subject information].

The instrumented socket was an ischial-containment (IC) socket with a flexible inner socket, using elastomeric suction suspension. Sensors strips were secured between the flexible inner socket and the exterior hard socket using adhesive tape [see Fig. 5]. Strips were placed with even spacing about the socket, however, due to length they were unable to extended to the distal most point of the socket. The strips were connected to a PCB with an inertial measurement unit and Bluetooth module, secured to the posterior side of the socket.

Data was collected from the sensors during standing and a short walking task. The participant was instructed to stand in a comfortable stance whilst a short portion of data was collected. They were then instructed to perform a short walk back and forth across the laboratory. The forward and return journey was repeated five times at a comfortable pace. The purpose of this task was to simulate walking conditions on a flat surface.

## V. Results

### A. Bench Tests

Data obtained from the experiments was analyzed offline using MATLAB. The resistances of three sensors were examined and demonstrated an average working resistance range of 33.33 MΩ to 5.72 kΩ. The resistance of the sensors decayed exponentially as the applied pressure increased [see Fig. 6]. Following the initial resistance drop, the sensors tended to produce a linear output over a narrow resistance range. Resistance values fluctuated upon repeat tests producing lower resistance values, suggestive of a cyclic drift.

Ten sensors were compared using Pearson's linear correlation coefficient (PLCC), providing a value between +1 and -1, where +1 is complete linear correlation, 0 is no linear correlation and -1 is complete negative linear correlation. The results of this analysis are displayed in Table 2. Each of the sensors was loaded cyclically for twenty cycles from which an average response was obtained for comparison. The coefficients indicate a high positive linearity for a selection of the sensors, in particular sensors 3 and 4. There is significant variation in linearity when comparing all ten of the tested sensors. The mean linear correlation coefficient was 0.9185.

Six sensors were subjected to 20 cyclical loads from which an average response was used for calibration, followed by

discrete loading from which expected and calculated values of pressure were obtained. Linear, polynomial and exponential relationships were fitted to the sensor response curve. Further discrete loading and unloading at intervals of 40 kPa between 0 and 400 kPa was performed, from which accuracy errors were determined.

Table 3 summarizes the sensors, their lowest error model and the associated accuracy error. Polynomial models appeared to produce the lowest errors in calculated pressure with first order linear equations commonly producing greater accuracy. Despite a linear model tending to produce the lowest errors, the magnitude of these errors were deemed unacceptable for the intended loading range. The minimum errors across the six sensors tested amounted to approximately 64 kPa or 16% of the full-scale range.

Fig. 7 displays the raw sensor voltage ranges for three sensors tested on a complaint surface intended to mimic the environment of the sensors' intended use. The diagram indicates an upward cyclic drift for each of the sensors with an element of random variability, particularly prominent in the response of sensor 1. The drift corresponded to 0.0053 V/cycle, accumulating to a total of 1.06 V over the 200 cycles applied. The presence of cyclic drift was unaffected by use of the stiffer backing material producing an average value of 0.00715 V/cycle or a total of 1.43 V over the 200 cycles applied. The harder backing material also led to a 13% increase in the sensor output voltage range as compared to the softer material. This effect is potentially the result of the lower load relief offered by the harder surface. Random fluctuations atop the drift were noted and may be caused by the syringe head sliding. This would lead to an additional shear effect. Further work is required to determine if a refined loading arrangement is required.

An element of static drift was recorded from the four tested sensors. The magnitude of the drift appeared dependent on the magnitude of the load and as such, the portion of sensor response curve active. A higher drift was detected during the 25kPa load and a minimal drift was recorded at 100 kPa [see Table 4 for the values for each of the loading thresholds].

A short time delay was discovered between the application of maximal load and the maximum output voltage of the sensor, possibly resulting from the static drift of the sensor. An average delay of approximately 0.22 seconds was obtained for the six sensors tested. The compliance of the backing material appeared to have no effect on the duration of this delay.

The sensor response for each of the tested loading rates were cross-correlated. Minor variations were detected between sensor response on repeat measurements, however, no clear relationship was determined between these variations and loading rate.

Loading and unloading responses were averaged for twenty loading cycles, the average case was compared for loading and unloading. Hysteresis error was determined as the greatest difference between loading and unloading response as a percentage of the FSO. The hysteresis errors observed are displayed in Table 5.

The effect of heat on sensor response was examined for ten sensors. Zero-load thermal response tests indicated fluctuation in resting sensor output across the temperature thresholds as characterized by sensor response standard deviation in Table 6.

Comparison of the differences between starting and ending voltages indicated a non-statistically significant relationship between temperature and zero-load response (p-value of 0.150). Cyclic testing revealed an alteration in signal form as the temperature was increased [see Fig. 8]. Loading response at half-load (200kPa) was taken for twenty cycles at temperatures 20°C, 30°C and 40°C for each sensor. These values were compared and indicated a statistically significant relationship (p-value of 0.000) between each of the thresholds as the temperature increased. However, there was considerable variation between sensors, displaying four different relationships across the three temperature thresholds. The mean voltages at 200 kPa are shown in Table 7.

### B. Participant Evaluation

Participant data was obtained for standing and walking tasks. Inertial measurement data from the PCB was used to detect stance and swing-phase. Pressure maps of the socket were developed from the sensor data. Individual sensor output was normalized across both tasks. As such, each block of the pressure map represents a sensor's instantaneous observed pressure in relation to its maximum and minimum observed pressures.

Results from the standing task indicate predominantly high loading close to each sensor's maximum observed pressure across the majority of socket, except for the lower-right portion (posterior and lateral sections) of the residual limb.

During walking swing-phase, low loading was perceived across the majority of the sensors in the socket with a concentration of mid-level loads towards the distal-anterior, distal medial and proximal-most rims of the socket.

The walking stance pressure was notably lower across the socket than the standing pressure, the load is also distributed more evenly across the socket.

## VI. Discussion

### A. Bench Tests

A thin, flexible piezo-resistive pressure sensor was designed, fabricated and evaluated within a loading range of 0 to 400kPa based on the use of Velostat. The sensor is intended for use within a prosthetic socket, providing an indication of stump-socket interface pressures. Fabrication of the sensor utilizes readily available materials and printed circuit board manufacturing techniques to develop bespoke sensor designs. Sensor size and shape can be easily altered allowing individualized designs to be produced in addition to inclusion of numerous sensors through utilization of multiplexing.

Experimental tests were performed to evaluate the sensor performance between 0 to 400 kPa pressures, encompassing typical reported loading within the socket. The sensors exhibited a mixture of linear and non-linear responses to applied pressure depending on the sensing element examined. Poor sensor repeatability was noted due to a cyclic drift contributing to large sensor inaccuracy and poor precision. Cyclic drifts of up to 0.00715 V/cycle were recorded for a 0 to

3.3V power supply range. These issues may stem from the viscoelastic properties of the polyolefin polymer and agglomeration of the carbon particles distributed within it [66].

The magnitude of the cyclic drift decayed exponentially with subsequent cycles. Large errors were produced by initial repetitions. This finding suggests that the sensors must be loaded for many cycles before attempting to fit a calibration model to them. This process would demand a significant amount of time, requiring each sensor to be calibrated individually due to the vast differences in the nature of the output response.

Generally, linear models led to the lowest calibration errors, despite at times larger RMSE during the initial fit. Attempts to fit the sensor response with an exponential form further exacerbated the accuracy error. It is surmised that the large accuracy errors tie into the poor precision of the sensors and the tendency for the response to vary on subsequent cycles. It is possible that the sensors might also be approximated with a more complicated viscoelastic model such as a Maxwell material, however, this would require examination of the strain response during loading and its relation to the material's electrical characteristics.

A static drift of up to 1.17%/min of the full-scale output (FSO) was observed during stationary tests. A hysteresis effect was observed, with the greatest error being 7.25% of the full-scale output (FSO). The sensors were tested at different loading rates which appeared to produce negligible effect on response.

Zero-load thermal drift tests indicated fluctuation in sensor response, however, no discernable pattern was obtained from this data suggesting limited influence of temperature on the resting sensor voltage. Under cyclical loading the sensors exhibited variation in response under load across the temperature range. The lack of difference at zero-load may be a result of the high internal resistance of the material. This resistance drops significantly upon loading, after which temperature influences the response. Four different relationships were observed between temperature and voltage dependent on the sensor tested. This suggests that a single model cannot be applied to all sensors, problematic when attempting to compensate for temperature within the expected body-heat range. A limitation of this test was the number of cycles applied to the sensors, longer tests were avoided due to the inconsistency in the relationship between temperature and voltage response across sensors.

### B. Participant Evaluation

The sensor output during standing, walking stance-phase and walking swing-phase displayed considerably different patterns as observed in Fig. 9.

The load distribution observed during the standing task aligns with loading expectations for an ischial-containment socket in which the weight is typically borne as a combination of hydrostatic and ischial weight bearing [67]. The lack of loading towards the posteriors and lateral sections of the socket are suggestive of a forward-leaning posture.

During walking swing-phase low loading was observed across the socket with mid-level loads at distal and proximal-most regions. Loading is expected towards the distal end of the socket during swing-phase due to suction suspension acting on the residual limb. The higher concentration of loading towards the anterior and medial sections may be attributed to the gravitational component of socket weight acting on the residuum. The loading at the posterior proximal rim may be reflective of gluteal muscle engagement as the limb is rotated.

Walking stance pressure displayed evenly distributed loading across the socket at a lower threshold that that observed during standing. Walking is a dynamic motion and as such, even loading is expected as load is transferred from the back to the front of the socket as the foot rolls over the heel during mid-stance.

The formation of these pressure maps enables a method of real-time visual feedback which may be used in the production of prosthetic sockets, or the examination of gait characteristics by prosthetists and physiotherapists respectively. Whilst the system cannot provide an accurate measure of the pressures in the socket in its current state, it can be used to determine contact patterns allowing assessment of load targeting, important for maintaining residuum health and avoiding the formation of conditions such as pressure sores.

## VII. Conclusion

The results demonstrate that despite advantages in relation to low cost, low profile and ease of integration, Velostat has numerous shortfalls with regards to accuracy and precision when used as a pressure sensitive transducer. Accuracy errors were recorded in the range of 16% to 48% of the full-scale output depending on the sensor tested. Thermal response tests indicated a variation in the voltage range of the sensor of up to 67% of the ambient temperature voltage range. It may be possible to model many of the effects of factors such as drift, cyclic drift and thermal response, however, accounting for the large number of variables affecting output would demand significant computation that may affect real-time capability necessary for clinical utility. Furthermore, this would require many test cycles for each sensor, impractical when using a large number of sensors.

Whilst the outlined design is not suitable for obtaining accurate measures of pressure, it does have the potential to determine contact between the residual limb and the socket as evidenced in the participant study. Distinct loading patterns were observed within the socket during standing and walking phases, appearing to align with expected load distribution for an IC socket. This information may be used to prosthetists as a fitting tool when constructing new sockets, particularly with regards to specific-surface bearing (SSB) designs to confirm the implications of socket form adjustments.

## Acknowledgment

This work was conducted under the auspices of the Royal British Legion Centre for Blast Injury Studies at Imperial College London. The authors would like to acknowledge the financial support of the Royal British Legion. We would like to acknowledge the Holderness Limb Fitting Centre for their input and feedback.

## REFERENCES


[1] K. Ziegler-Graham, E.J. MacKenzie, P.L. Ephraim, T.G. Travison, and R. Brookmeyer, "Estimating the Prevalence of Limb Loss in the United States: 2005 to 2050.," *Archives of Physical Medicine and Rehabilitation*. vol. 89, no. 3, pp. 422–429, 2008.

[2] Y. Izumi, K. Satterfield, S. Lee, and L. Harkless, "Risk of Reamputation in Diabetic Patients.," *Diabetes Care*. vol. 29, pp. 566–570, 2006.

[3] T.R. Dillingham, L.E. Pezzin, and A.D. Shore, "Reamputation, mortality, and health care costs among persons with dysvascular lower-limb amputations.," *Archives of Physical Medicine and Rehabilitation*. vol. 86, no. 3, pp. 480–486, 2005.

[4] A. Eshraghi, N.A. Abu Osman, H. Gholizadeh, S. Ali, and W.A.B.W. Abas, "Interface stress in socket/residual limb with transtibial prosthetic suspension systems during locomotion on slopes and stairs.," *American Journal of Physical Medicine and Rehabilitation*. vol. 94, no. 1, pp. 1–10, 2015.

[5] D.S. Edwards, R.D. Phillip, N. Bosanquet, A.M.J. Bull, and J.C. Clasper, "What Is the Magnitude and Long-term Economic Cost of Care of the British Military Afghanistan Amputee Cohort?," *Clinical Orthopaedics and Related Research*. vol. 473, no. 9, pp. 2848–2855, 2015.

[6] Ministry of Defence, *Afghanistan and Iraq Amputation Statistics 7 October 2001 – 31 March 2017*., 2017.

[7] F. Wang, Y. Qi, S. Wen, and C. Wu, "Intelligent bionic leg motion estimation based on interjoint coordination using PCA and RBF neural networks.," *2012 IEEE International Conference on Mechatronics and Automation, ICMA 2012*. pp. 311–315, 2012.

[8] F. Zhang, M. Liu, and H. Huang, "Preliminary study of the effect of user intent recognition errors on volitional control of powered lower limb prostheses.," *Proceedings of the Annual International Conference of the IEEE Engineering in Medicine and Biology Society, EMBS*. pp. 2768–2771, 2012.

[9] D.M. Sengeh and H. Herr, "A variable-impedance prosthetic socket for a transtibial amputee designed from magnetic resonance imaging data.," *Journal of Prosthetics and Orthotics*. vol. 25, no. 3, pp. 129–137, 2013.

[10] C.C. Nielson, "A Survey of Amputees: Functional Level and Life Satisfaction, Information Needs, and the Prosthetist's Role,." *Journal of Prosthetics and Orthotics*. vol. 3, no. 3, pp. 125–129, 1991.

[11] L. Paternò, M. Ibrahimi, E. Gruppioni, A. Menciassi, and L. Ricotti, "Sockets for limb prostheses: A review of existing technologies and open challenges.," *IEEE Transactions on Biomedical Engineering*. vol. 65, no. 9, pp. 1996–2010, 2018.

[12] T. Dillingham, L. Pezzin, E. MacKenzie, and A. Burgess, "Use and Satisfaction with Prosthetic Devices Among Persons with Trauma-Related Amputations: A Long-Term Outcome Study.," *American Journal of Physical Medicine & Rehabilitation*. vol. 38, no. 2, pp. 563–571, 2001.

[13] A.F.T. Mak, M. Zhang, and D.A. Boone, "State-of-the-art research in lower-limb prosthetic biomechanics-socket interface: A review.," *Journal of Rehabilitation Research and Development*. vol. 38, no. 2, pp. 161–173, 2001.

[14] H.E. Meulenbelt, J.H. Geertzen, M.F. Jonkman, and P.U. Dijkstra, "Determinants of Skin Problems of the Stump in Lower-Limb Amputees.," *Archives of Physical Medicine and Rehabilitation*. vol. 90, no. 1, pp. 74–81, 2009.

[15] H.E.J. Meulenbelt, P.U. Dijkstra, M.F. Jonkman, and J.H.B. Geertzen, "Skin problems in lower limb amputees: A systematic review.," *Disability and Rehabilitation*. vol. 28, no. 10, pp. 603–608, 2006.

[16] J.E. Sanders, S.G. Zachariah, A.K. Jacobsen, and J.R. Fergason, "Changes in interface pressures and shear stresses over time on trans-tibial amputee subjects ambulating with prosthetic limbs: Comparison of diurnal and six-month differences.," *Journal of Biomechanics*. vol. 38, no. 8, pp. 1566–1573, 2005.

[17] J.E. Sanders, "Thermal response of skin to cyclic pressure and pressure with shear: A technical note.," *Journal of Rehabilitation Research and Development*. vol. 37, no. 5, pp. 511–515, 2000.

[18] J.T. Highsmith and T. Jason, "Identifying and Managing Skin Issues With Lower-Limb Prosthetic Use.," *inMotion - A Publication of the Amputee Coalition*. vol. 21, no. 1, pp. 41–43, 2011.

[19] S. Ali, N.A. Abu Osman, A. Eshraghi, H. Gholizadeh, N.A. Bin Abd Razak, and W.A.B. Bin Wan Abas, "Interface pressure in transtibial socket during ascent and descent on stairs and its effect on patient satisfaction.," *Clinical Biomechanics*. vol. 28, no. 9–10, pp. 994–999, 2013.

[20] O. Yildirim and L.E. Ostrander, "Assessing socket differences in fitting prosthesis to residual limb.," *Bioengineering, Proceedings of the Northeast Conference*. vol. 1, pp. 61–63, 1998.

[21] A.W.P. Buis and P. Convery, "Calibration problems encountered while monitoring stump/socket interface pressures with force sensing resistors: Techniques adopted to minimise inaccuracies.," *Prosthetics and Orthotics International*. vol. 21, no. 3, pp. 179–182, 1997.

[22] A.A. Polliack, R.C. Sieh, D.D. Craig, S. Landsberger, D.R. McNeil, and E. Ayyappa, "Scientific validation of two commercial pressure sensor systems for prosthetic socket fit.," *Prosthetics and Orthotics International*. vol. 24, no. 1, pp. 63–73, 2000.

[23] A. Hollinger and M.M. Wanderley, "Evaluation of Commercial Force-Sensing Resistors.," In: *International Conference on New Interfaces for Musical Expression*. pp. 1–4. , Paris (2006).

[24] A.M. El-Sayed, N.A. Hamzaid, and N.A.A. Osman, "Piezoelectric bimorphs' characteristics as in-socket sensors for transfemoral amputees,." *Sensors (Switzerland)*. vol. 14, no. 12, pp. 23724–23741, 2014.

[25] F. Jasni, N.A. Hamzaid, A.G.A. Muthalif, Z. Zakaria, H.N. Shasmin, and S.C. Ng, "In-Socket Sensory System for Transfemoral Amputees Using Piezoelectric Sensors: An Efficacy Study.," *IEEE/ASME Transactions on Mechatronics*. vol. 21, no. 5, pp. 2466–2476, 2016.

[26] M. Rossi, M. Nardello, L. Lorenzelli, and D. Brunelli, "Dual mode pressure sensing for prosthetic interfaces.," *Proceedings - 2017 7th International Workshop on Advances in Sensors and Interfaces, IWASI 2017*. pp. 109–114, 2017.

[27] A.A. Polliack, D.D. Craig, R.C. Sieh, S. Landsberger, and D.R. McNeal, "Laboratory and clinical tests of a prototype pressure sensor for clinical assessment of prosthetic socket fit.," *Prosthetics and Orthotics International*. vol. 26, no. 1, pp. 23–34, 2002.

[28] K. Sundara-Rajan, A. Bestick, G.I. Rowe, et al., "An interfacial stress sensor for biomechanical applications.," *Measurement Science and Technology*. vol. 23, no. 8, p. 2012.

[29] X. Lü, K. Sundara-Rajan, W. Lu, and A. V. Mamishev, "Transfer function of interfacial stress sensor for artificial skin applications.," *IEEE Transactions on Electron Devices*. vol. 60, no. 8, pp. 2640–2647, 2013.

[30] P. Laszczak, L. Jiang, D.L. Bader, D. Moser, and S. Zahedi, "Development and validation of a 3D-printed interfacial stress sensor for prosthetic applications.," *Medical Engineering and Physics*. vol. 37, no. 1, pp. 132–137, 2015.

[31] G.T. Kanellos, G. Papaioannou, D. Tsiokos, C. Mitrogiannis, G. Nianios, and N. Pleros, "Two dimensional polymer-embedded quasi-distributed FBG pressure sensor for biomedical applications.," *Optics Express*. vol. 18, no. 1, p. 179, 2010.

[32] D. Tsiokos, G.T. Kanellos, G. Papaioannou, and S. Pissadakis, *Fiber Optic–Based Pressure Sensing Surface for Skin Health Management in Prosthetic and Rehabilitation Interventions*., 2016.

[33] Zhi Feng Zhang, Xiao Ming Tao, Hua Peng Zhang, and Bo Zhu, "Soft fiber optic sensors for precision measurement of shear stress and pressure.," *IEEE Sensors Journal*. vol. 13, no. 5, pp. 1478–1482, 2013.

[34] E.A. Al-Fakih, N.A.A. Osman, A. Eshraghi, and F.R.M. Adikan, "The capability of fiber Bragg grating sensors to measure amputees' trans-tibial stump/socket interface pressures," *Sensors (Switzerland)*. vol. 13, no. 8, pp. 10348–10357, 2013.

[35] J. Missinne, E. Bosman, B. Van Hoe, G. Van Steenberge, P. Van Daele, and J. Vanfleteren, "Embedded flexible optical shear sensor.," *Proceedings of IEEE Sensors*. pp. 987–990, 2010.

[36] L.S. Lincoln, M. Quigley, B. Rohrer, C. Salisbury, and J. Wheeler, "An optical 3D force sensor for biomedical devices.," *Proceedings of the IEEE RAS and EMBS International Conference on Biomedical Robotics and Biomechatronics*. pp. 1500–1505, 2012.

[37] J. Wheeler, A. Mazumdar, L. Marron, K. Dullea, J. Sanders, and K. Allyn, "A pressure and shear sensing liner for prosthetic sockets.," *Proceedings of the Annual International Conference of the IEEE Engineering in Medicine and Biology Society, EMBS*. vol. 2016-Octob, pp. 2026–2029, 2016.

[38] M.C. Hsieh, Y.K. Fang, M.S. Ju, et al., "A contact-type piezoresistive micro-shear stress sensor for above-knee prosthesis application.," *Journal of Microelectromechanical Systems*. vol. 10, no. 1, pp. 121–127, 2001.

[39] J.W. Wheeler, J.G. Dabling, D. Chinn, et al., "MEMS-based bubble pressure sensor for prosthetic socket interface pressure measurement.," *Proceedings of the Annual International Conference of the IEEE Engineering in Medicine and Biology Society, EMBS*. pp. 2925–2928, 2011.

[40] L. Lorenzelli, G. Sordo, A. Bagolini, and G. Resta, "Socketmaster: Integrated sensors system for the optimised design of prosthetic socket for above knee amputees.," *Proceedings - 2017 1st New Generation of CAS, NGCAS 2017*. no. 645239, pp. 233–236, 2017.

[41] J.K. Lee, N. Stoffel, and K. Fite, "Electronic packaging of sensors for lower limb prosthetics.," *Proceedings - Electronic Components and Technology Conference*. no. Ecoflex 0050, pp. 86–91, 2012.

[42] A.M. Almassri, W.Z. Wan Hasan, S.A. Ahmad, et al., "Pressure sensor: State of the art, design, and application for robotic hand.," *Journal of Sensors*. vol. 2015, p. 2015.

[43] M.I. Tiwana, S.J. Redmond, and N.H. Lovell, "A review of tactile sensing technologies with applications in biomedical engineering.," *Sensors and Actuators, A: Physical*. vol. 179, pp. 17–31, 2012.

[44] P. Saccomandi, E. Schena, C.M. Oddo, L. Zollo, S. Silvestri, and E. Guglielmelli, "Microfabricated tactile sensors for biomedical applications: A review.," *Biosensors*. vol. 4, no. 4, pp. 422–448, 2014.

[45] E.A. Al-Fakih, N.A. Abu Osman, and F.R. Mahmad Adikan, *Techniques for interface stress measurements within prosthetic sockets of transtibial amputees: A review of the past 50 years of research*., 2016.

[46] S. Poeggel, D. Tosi, D. Duraibabu, G. Leen, D. McGrath, and E. Lewis, "Optical fibre pressure sensors in medical applications.," *Sensors (Switzerland)*. vol. 15, no. 7, pp. 17115–17148, 2015.

[47] V. Mishra, N. Singh, U. Tiwari, and P. Kapur, "Fiber grating sensors in medicine: Current and emerging applications.," *Sensors and Actuators, A: Physical*. vol. 167, no. 2, pp. 279–290, 2011.

[48] S. Salibindla, B. Ripoche, D.T.H. Lai, and S. Maas, "Characterization of a new flexible pressure sensor for body sensor networks.," *Proceedings of the 2013 IEEE 8th International Conference on Intelligent Sensors, Sensor Networks and Information Processing: Sensing the Future, ISSNIP 2013*. vol. 1, pp. 27–31, 2013.

[49] J.H. Low, P.M. Khin, and C.H. Yeow, "A pressure-redistributing insole using soft sensors and actuators.," *Proceedings - IEEE International Conference on Robotics and Automation*. vol. 2015-June, no. June, pp. 2926–2930, 2015.

[50] G.R. Hurley, A.C. Pedtke, N.C.R. Smith, et al., "Prosthetic sockets with sensors," (2017).

[51] E. Jeong, J. Lee, and D.E. Kim, "Finger-gesture recognition glove using velostat (ICCAS 2011).," *International Conference on Control, Automation and Systems*. no. Iccas, pp. 206–210, 2011.

[52] D. Giovanelli and E. Farella, "Force Sensing Resistor and Evaluation of Technology for Wearable Body Pressure Sensing.," *Journal of Sensors*. vol. 2016, p. 2016.

[53] B.W. Lee and H. Shin, "Feasibility Study of Sitting Posture Monitoring Based on Piezoresistive Conductive Film-Based Flexible Force Sensor.," *IEEE Sensors Journal*. vol. 16, no. 1, pp. 15–16, 2016.

[54] R. Barba, Á.P. De Madrid, and J.G. Boticario, "Development of an inexpensive sensor network for recognition of sitting posture.," *International Journal of Distributed Sensor Networks*. vol. 2015, p. 2015.

[55] L. Harris and M. Oliver, "Design and Fabrication of a Piezoresistive Tactile Sensor for Ergonomic Analyses Design and Fabrication of a Piezoresistive Tactile Sensor for Ergonomic Analyses A Thesis Presented to : The Faculty of Graduate Studies The University of Guelph By : For the," (2014).

[56] M. Vega-Barbas, I. Pau, J. Ferreira, E. Lebis, and F. Seoane, "Utilizing smart textiles-enabled sensorized toy and playful interactions for assessment of psychomotor development on children.," *Journal of Sensors*. vol. 2015, no. May, p. 2015.

[57] R. Van Donselaar and W. Chen, "Design of a smart textile mat to

study pressure distribution on multiple foam material configurations.," *ACM International Conference Proceeding Series*. pp. 0–4, 2011.

[58] M. Kalantari, J. Dargahi, J. Kövecses, M.G. Mardasi, and S. Nouri, "A new approach for modeling piezoresistive force sensors based on semiconductive polymer composites.," *IEEE/ASME Transactions on Mechatronics*. vol. 17, no. 3, pp. 572–581, 2012.

[59] Z. Del Prete, L. Monteleone, and R. Steindler, "A novel pressure array sensor based on contact resistance variation: Metrological properties.," *Review of Scientific Instruments*. vol. 72, no. 2, pp. 1548–1553, 2001.

[60] J. Tolvanen, J. Hannu, and H. Jantunen, "Hybrid foam pressure sensor utilizing piezoresistive and capacitive sensing mechanisms.," *IEEE Sensors Journal*. vol. 17, no. 15, pp. 4735–4746, 2017.

[61] E. Boutwell, R. Stine, A. Hansen, K. Tucker, and S. Gard, "Effect of prosthetic gel liner thickness on gait biomechanics and pressure distribution within the transtibial socket.," *The Journal of Rehabilitation Research and Development*. vol. 49, no. 2, p. 227, 2012.

[62] G.K. Klute, E. Huff, and W.R. Ledoux, "Does activity affect residual limb skin temperatures?," *Clinical orthopaedics and related research*. vol. 472, no. 10, pp. 3062–3067, 2014.

[63] N. Mathur, I. Glesk, and A. Buis, "Skin temperature prediction in lower limb prostheses.," *IEEE Journal of Biomedical and Health Informatics*. vol. 20, no. 1, pp. 158–165, 2016.

[64] A.D. Segal and G.K. Klute, "Residual limb skin temperature and thermal comfort in people with amputation during activity in a cold environment.," *Journal of Rehabilitation Research and Development*. vol. 53, no. 5, pp. 619–628, 2016.

[65] L.E. Diment, M.S. Thompson, and J.H.M. Bergmann, "Comparing thermal discomfort with skin temperature response of lower-limb prosthesis users during exercise.," *Clinical Biomechanics*. vol. 69, no. July, pp. 148–155, 2019.

[66] Y. Li, X. Huang, L. Zeng, et al., "A review of the electrical and mechanical properties of carbon nanofiller-reinforced polymer composites.," *Journal of Materials Science*. vol. 54, no. 2, pp. 1036–1076, 2019.

[67] M.D. Muller, "Transfemoral Amputation: Prosthetic Management.," *Chapter 20B - Atlas of Limb Prosthetics: Surgical, Prosthetic, and Rehabilitation Principles*. pp. 103–115, 2004.

**Matthew Hopkins** received the BEng degree in mechanical engineering from the University of Southampton, Hampshire, UK, in 2012, the MSc degree in Cybernetics from the University of Reading, Berkshire, UK, in 2014 and the PhD degree in prosthetic sockets and sensor design from Imperial College London, UK, in 2019.

He is currently a Research Assistant with the Sackler MSk Laboratory in the Department of Surgery and Cancer at Imperial College London, UK. His research interests include development of sensors and sensing technology, wearable electronic systems and prosthetic devices.

**Ravi Vaidyanathan** (M'08) received the M.S. and PhD degrees in mechanical engineering from Case Western Reserve University, Cleveland, OH, in 1996 and 2001 respectively.

He is currently a Reader at Imperial College London, UK where he leads the Biomechatronics Laboratory. His research focuses on mechanisms of sensory-motor control, with focus on bio-robotics and human-robot interfaces.

Dr. Vaidyanathan's holds awards from SAGE Journals, the Institute of Electrical and Electronics Engineers (IEEE), American Institute of Aeronautics and Astronautics (AIAA), the Robotics Society of Japan (RSJ) and Institute of Engineering Technology (IET).

**Alison H. McGregor** qualified as a Physiotherapist in 1989, gaining an MSc degree in biomedical engineering from Surrey University, Surrey, U.K. and a PhD degree in spinal mechanics and low back pain from the Royal Postgraduate Medical School, London.

She became part of Imperial College in 1998 and obtained her Chair in 2009. Her research interests are in the area of low back pain and osteoarthritis, injury mechanisms, disease progression, and rehabilitation.

Professor McGregor's awards and honors include the ISSLS Clinical Prize in 2011 and the Backcare Award in 2012 for her clinical trial work. In addition, she won the Cochrane Back Review Group First Scientific Award for Best Review in relation to Rehabilitation following surgery for lumbar spinal stenosis 2014.

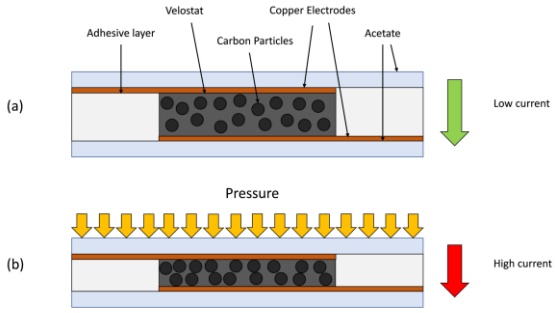


Fig. 1. Sensor construction, (a) unloaded, (b) loaded.

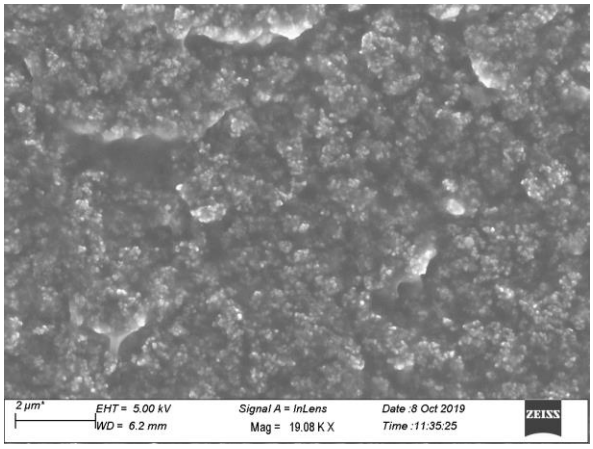


Fig. 2. SEM micrograph of a Velostat sample.

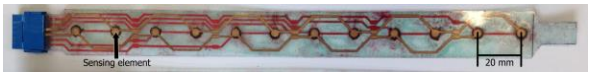


Fig. 3. Completed sensor strip featuring twelve sensitive elements.

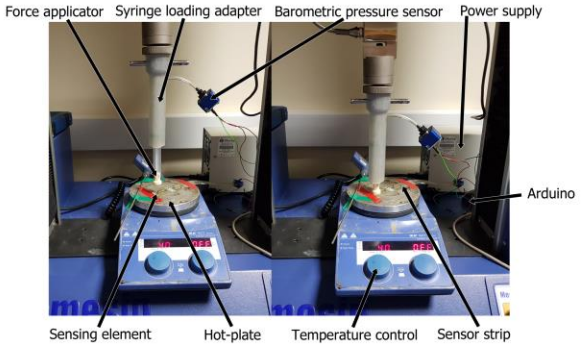


Fig. 4. The syringe loading adapter attached to the MecMesin machine head applying load to a sensor on a hot-plate. Left displays the syringe extended and right displays the syringe compressed.

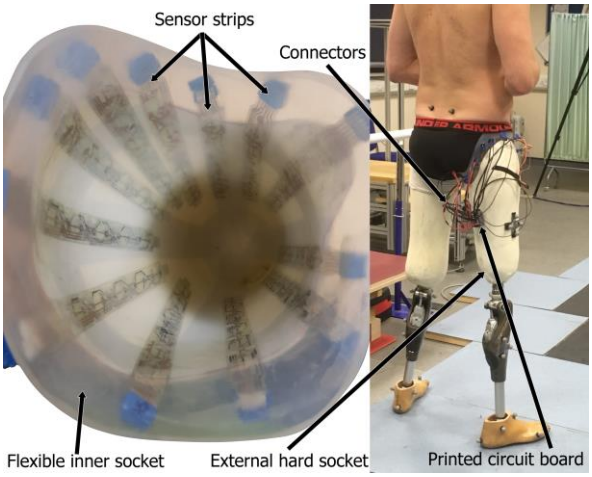


Fig. 5. Left: Arrangement of sensors within the socket. Right: Placement of the printed circuit board control unit relative to the socket.

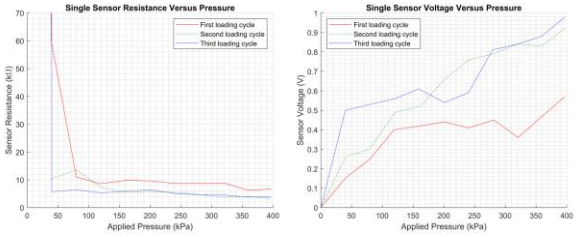


Fig. 6. Left: single sensor resistance response for three loading cycles. Right: corresponding sensor voltage output.

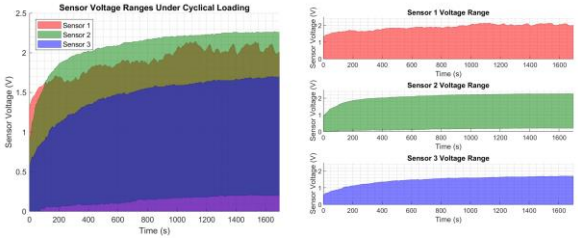


Fig. 7. Raw sensor data for three sensors loaded between 0 and 400 kPa for 200 cycles on a compliant surface.

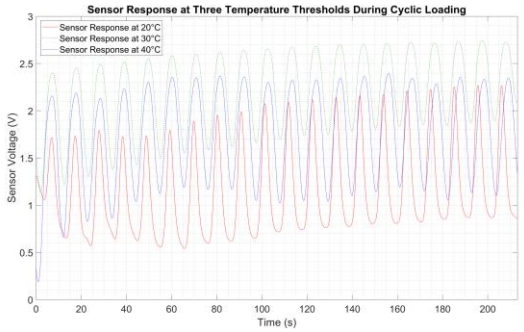


Fig. 8. Temperature response from a single sensor at three temperature thresholds.

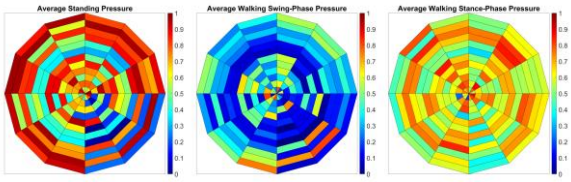


Fig. 9. Left to right: averages of standing pressure, walking swing-phase pressure and walking stance-phase pressure.

TABLE I
SUBJECT INFORMATION

| | |
|---|---|
| Amputation Type | Bilateral, through-knee and transfemoral. |
| Instrumented Leg | Right (transfemoral). |
| Age (years) | 32 |
| Sex | Male |
| Height (cm) | 190 |
| Weight with the prosthesis (kg) | 86.0 |
| Socket type (instrumented) | Ischial containment, hard-soft combination. |
| Liner type | Elastomeric suction. |
| Joint type | Genium knee. |

TABLE II
PEARSON'S LINEAR CORRELATION COEFFICIENT

| Sensor | 1 | 2 | 3 | 4 | 5 | 6 | 7 | 8 | 9 | 10 |
|---|---|---|---|---|---|---|---|---|---|---|
| Value | 0.92 | 0.84 | 0.98 | 0.99 | 0.94 | 0.89 | 0.91 | 0.94 | 0.91 | 0.86 |

TABLE III
CALIBRATION MODEL ERRORS

| Sensor | 1 | 2 | 3 | 4 | 5 | 6 |
|---|---|---|---|---|---|---|
| Lowest Error Model | 2nd Order Polynomial | 2nd Order Polynomial | Linear | Linear | Linear | Linear |
| Model Error (Mean) | 190 kPa | 151 kPa | 67 kPa | 64 kPa | 64 kPa | 125 kPa |

TABLE IV
STATIC DRIFT PROPERTIES

| Static Drift at 25kPa | Static Drift at 100kPa | Static Drift at 207kPa | Static Drift at 312kPa |
|---|---|---|---|
| 0.039 V/min | 0.015 V/min | 0.024 V/min | 0.027 V/min |
| 1.17 %/min | 0.45 %/min | 0.71 %/min | 0.82 %/min |

TABLE V
HYSTERESIS ERRORS

| Sensor | 1 | 2 | 3 | 4 | 5 | 6 |
|---|---|---|---|---|---|---|
| Hysteresis (%) | 1.92 | 1.47 | 3.10 | 7.25 | 5.05 | 4.32 |

TABLE VI
STANDARD DEVIATION OF UNLOADED SENSORS AT THREE THERMAL THRESHOLDS

| Temp\Sensor | 1 | 2 | 3 | 4 | 5 | 6 | 7 | 8 | 9 | 10 |
|---|---|---|---|---|---|---|---|---|---|---|
| 20°C | 2.06 | 2.07 | 0.41 | 0.39 | 2.24 | 1.48 | 0.76 | 0.73 | 0.55 | 0.48 |
| 30°C | 6.81 | 6.80 | 1.79 | 1.69 | 1.74 | 5.79 | 1.41 | 1.40 | 0.72 | 0.62 |
| 40°C | 2.82 | 2.80 | 0.75 | 0.55 | 1.33 | 2.33 | 0.62 | 0.55 | 0.62 | 0.53 |

TABLE VII
MEAN VOLTAGE AT HALF-LOAD (200kPa)

| Temp\Sensor | 1 | 2 | 3 | 4 | 5 | 6 | 7 | 8 | 9 | 10 |
|---|---|---|---|---|---|---|---|---|---|---|
| 20°C | 1.50 | 0.60 | 0.19 | 2.15 | 0.21 | 1.40 | 2.19 | 1.98 | 1.29 | 1.25 |
| 30°C | 2.51 | 1.33 | 1.68 | 2.14 | 1.43 | 2.04 | 2.35 | 2.08 | 1.22 | 0.88 |
| 40°C | 2.19 | 1.79 | 1.27 | 1.53 | 1.86 | 1.84 | 2.03 | 2.16 | 1.25 | 0.43 |